



A Non-orthogonal Random Access Scheme Based on NB-IoT

Dan Wang¹ · Yuanyuan Qu¹ · Yongli Fu¹ · Yanjuan Yang¹ · Qirong Chen¹

Published online: 10 December 2019

© Springer Science+Business Media, LLC, part of Springer Nature 2019

Abstract

Narrowband Internet of Things (NB-IoT) is a Quasi-5G technology that will provide coverage for massive number of low-power consumption applications. Hence, the potential massive random access (RA) users call for a new RA scheme. In this paper, based on the key ideas of non-orthogonal multiple access and successive interference cancellation, the NB-IoT non-orthogonal random access (NB-NORA) scheme has been proposed to provide a more effective access performance for NB-IoT system. Further, the RA preamble (MSG1) transmission collision probability and initial layer 3 message (MSG3) outage performances are analyzed based on stochastic geometry, which is compared with the traditional NB-IoT orthogonal random access (NB-ORA) scheme. Simulation results show that the maximum throughput of MSG1 within NB-NORA scheme is double that within NB-ORA scheme, and the successful RA probability of NB-NORA is increased by about 75%.

Keywords NB-IoT · Random access process · NOMA · SIC

1 Introduction

As one of the 5G Internet of Things technologies, the number of connected devices in NB-IoT is expected to reach 50,000 per cell in the future [1–5]. It is based on orthogonal frequency-division multiple access (OFDMA) with 180 kHz system bandwidth and just provide up to 48 preambles [6, 7]. In a burst scenario, the number of preambles is seriously insufficient, and it will lead to access difficulties for a user. Furthermore, a large number of retransmissions of preambles will not only bring waste of network resources and congestion, but also cause the serious power consumption of device.

In [8], the exact expression of Narrowband IoT (NB-IoT) physical RA channel (NPRACH) repetition value and successful access probability are proposed and their relationship with channel resource utilization is analyzed. It shows that the probability of successful access increases along with the number of preamble repetitions increase, but excessive repetitions also waste system resources. In order to improve RA preamble detection probability, an enhanced RA scheme was proposed in literature [9], in which the Base

✉ Dan Wang
swnucquwd@163.com

¹ School of Communication and Information Engineering, The Chongqing University of Posts and Telecommunications, Chongqing 400065, China

Stations (BS) utilize the difference of MSG1 arrived time to detect the colliding terminals. Furthermore, the BS transmit multiple RA responses for the colliding terminals. However, as the successful transmission of MSG1 increases, the limited Narrowband Physical Uplink Shared Channel (NPUSCH) resources may be another bottleneck for RA process.

Non-orthogonal multiple access (NOMA) can achieve high spectral efficiencies by combining superposition coding at the transmitter and successive interference cancellation (SIC) at the receivers [10–12]. The probability of successful uplink transmission with NOMA in 5G was modeled and analyzed in [13]. Recently, NOMA researches only focus on LTE-A or 5G enhance Mobile Broadband (e-MBB) RA process [14, 15]. Compared to broadband transmission, the application scenario of NB-IoT has been changed and the system of NB-IoT has been redesigned. Therefore, a NB-IoT Non-Orthogonal Random Access (NB-NORA) mechanism has been proposed in this paper. In contrast to NB-IoT orthogonal random access (NB-ORA) scheme, NB-NORA transmit initial layer 3 message (MSG3) of collided terminals within same time–frequency resource instead of MSG1 retransmission, which can solve the resource bottleneck of NPUSCH effectively. Additionally, the information of terminal locations and channel conditions is utilized to improve performance of NOMA. In this paper, the probability of successful separation of collision preambles and successful MSG3 decoding based on NOMA are modeled and analyzed. Moreover, the influence of the power back off step size and repetition coding times on the success rate of access was investigated. Simulation results show, the maximum throughput of MSG1 is double that of NB-ORA and the maximum throughput of RA process (RAP) is increased by more than 75% in the proposed scheme.

This paper is organized as follows. Section 2 presents the NB-NORA mechanism description. The theoretical model of the proposed NB-NORA is analyzed detailed in Sect. 3. Simulation results are given in Sects. 4 and 5 concludes this paper.

2 NB-NORA Mechanism

In this section, the detailed description of the NB-NORA mechanism was given. The main steps are as follows: (A) The terminals transmit a RA preamble, then the BS detects and separates the colliding terminals, and captures Timing Advance (TA) of each terminal; (B) The BS send back MSG2 Narrowband Non-Orthogonal Multiple Access-Random Access Responses (NB-NORA-RARs); (C) The terminals estimate TA according to the power of a Narrowband Positioning Reference Signal. Based on the estimated TA, each terminal obtains its own RA response information by searching the closest TA value in the NB-NORA-RARs. The terminals transmit MSG3 on the NPUSCH according to the power configuration contained in MSG2; (D) The BS send contention resolution message (MSG4). The specific process is shown in Fig. 1.

2.1 RA Preamble (MSG1) Transmission and Detection

Sometimes, there are more than one terminal sending same MSG1 to BS simultaneously. In conventional NB-ORA, colliding terminals cannot be distinguished. Hence, BS only answer to the terminals with strongest received power by MSG2. The signal from terminals may go through different paths and result in a difference arrival time. If the cell size is more than twice the maximum delay spread, the BS may be able to differentiate the MSG1 transmitted from different terminals simultaneously and calculate TA based on the time of

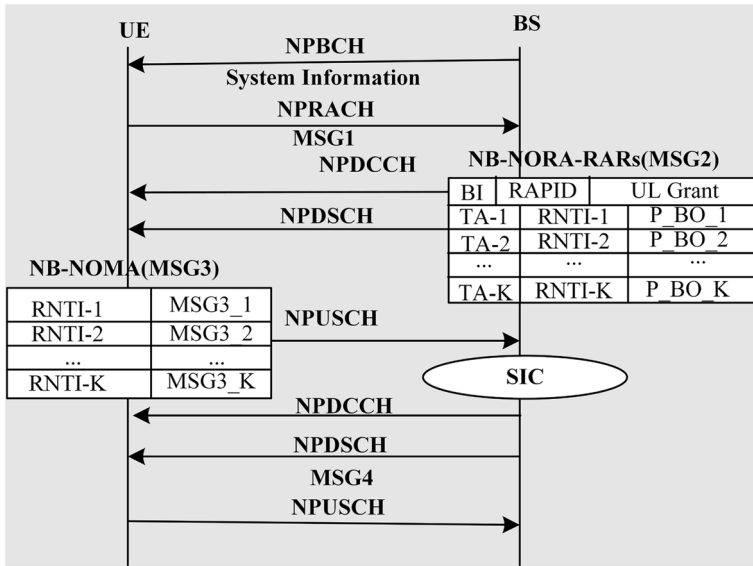


Fig. 1 NB-NORA process

arrival [16, 17]. Hence, BS will detect different colliding terminals and estimate their TAs by received MSG1s in NB-NORA.

2.2 NB-NORA-RARs (MSG2) Transmission and Detection

As shown in Fig. 1, unlike the traditional NB-RAR, the BS assembles NB-NORA-RARs in MSG2 of NB-NORA, which includes many RARs sets of TA, RNTI and P_BO. Each RAR set respond to one of the colliding terminals. Each terminal estimates their TA based on power of the received NPRS and then they receive the MSG2 from BS and pick up their own RAR set by searching for the nearest TA value in the NB-NORA-RARs group.

2.3 Initial Layer 3 Message (MSG3) Transmission and Detection

The NB-ORA uplink power control scheme attempts to maintain constant received power at BSs from different terminals. However, multiplexed MSG3 from different terminals with constant received power cannot be decoded separately, and lead to access fails. Therefore, in NB-NORA the NOMA technology is introduced into MSG3 transmission process, and BS can detect multiplexed MSG3 with different received power based on the SIC technology. The P-BO in the NB-NORA-RARs will indicates the decoding order of the terminals in the NB-NORA group. Obviously, the NOMA based MSG3 scheme can improve successful receipt of MSG3 and rate of successful access largely.

2.4 Contention Resolution Message (MSG4)

The last step of the NB-NORA mechanism is a contention resolution. After receiving Msg3 successfully, BS responds with a contention resolution tag as NB-ORA. If the terminal

does not receive a response from the base station before the timer expires, it leads to access fail.

3 Analytical Model for NB-NORA Process

3.1 Modeling for MSG1 Transmission and Detection

3.1.1 Separation Probability of NB-NORA Terminals

Let N denotes the total number of available preambles in a NB-IoT RA slot. Consider a specific preamble r , k is the number of terminals selected r preamble. Y_r^k be a random variable which takes value 1 if the preamble is used by exactly k out of m terminals and 0 otherwise.

$$E[Y_r^k] = \binom{m}{k} \frac{1}{N^k} \left(1 - \frac{1}{N}\right)^{m-k} \tag{1}$$

Define any two terminals time of arrivals interval is Δt , $c = 3 \times 10^8$ m/s is the speed of light d_j expresses the distance between BS and the j th terminal. The terminals are assumed to be uniformly distributed in the cell with radius d_c , thus the distribution of Δt can be computed and given by [14]

$$\begin{aligned} \Delta t &= \frac{|d_i - d_j|}{c}, \quad i \neq j; \quad f_{\Delta t}(x) = \frac{2x}{d_c^2}, \quad 0 < x < d_c \\ f_{\Delta t}(y) &= \frac{4c}{3d_c^4} (2d_c^3 - 3d_c^2cy + c^3y^3), \quad 0 < y < \frac{d_c}{c} \end{aligned} \tag{2}$$

t_{rms} is the root-mean-squared delay spread (RDS) of the channel. The probability p_S^{ij} that any two colliding terminals i, j can be separated is as shown in Eq. (3). The probability that all m terminals within same resource are successfully separated as Eq. (4)

$$\begin{aligned} P_S^{ij} &= P\{\Delta t_{ij} \geq t_{rms}\} \quad \forall i, j, \quad i \neq j, \quad i \in \{1, \dots, m\}, \quad j \in \{1, \dots, m\} \\ &= 1 - P\{\Delta t < t_{rms}\} \\ &= 1 - \int_0^{t_{rms}} f_{\Delta t}(y) dy \\ &= 1 - \frac{4c}{3d_c^4} \left(2d_c^3 t_{rms} - \frac{3}{2} d_c^2 c t_{rms}^2 + \frac{1}{4} c^3 t_{rms}^4 \right) \end{aligned} \tag{3}$$

$$P^{sm} = P\{\Delta t_{ij} \geq t_{rms}\} \geq \prod P_S^{ij}, \quad \forall i, j, \quad i \neq j, \quad i \in \{1, \dots, m\}, \quad j \in \{1, \dots, m\} \tag{4}$$

3.1.2 Number of Terminals Successfully Transmitting MSG1

The expectation of number of successful MSG1 access in NB-NORA scheme and NB-ORA scheme are Eqs. (5) and (6), respectively.

$$E[S]_{\text{NB-NORA}} = N(E[Y_r^1] + \dots + p^{sk} E[Y_r^k] + \dots + p^{sm} E[Y_r^m]) \tag{5}$$

$$E[S]_{\text{NB-ORA}} = m \left(1 - \frac{1}{N}\right)^{m-1} \tag{6}$$

Take $d_c = 2500$ m, $t_{rms} = 1$ μ s. Assumed the terminals select the preambles under 0–1 distribution and the total number of different preambles is $N = 48$, the throughput of successful transmitted MSG1 with orthogonal and non-orthogonal schemes are expressed respectively in Fig. 2.

From Fig. 2, when the multiplexing maximum value is 2, i.e., the maximum number of colliding terminals is 2 the maximum throughput of MSG1 transmission in NB-NORA can be increased by 40% compared with NB-ORA. When the multiplexing maximum value is 10, the maximum throughput of MSG1 transmission can be doubled. In addition, due to the limitation of the number of preambles, the throughput of NB-ORA reaches maximum when the number of users matches the number of preambles, while it of NB-NORA occurs in more users because it can distinguish multiple colliding terminals.

3.2 Modeling for MSG3 Transmission and Detection

After successful transmission of MSG1 and MSG2, the NOMA transmission of MSG3 and the decoding based on SIC technology are performed.

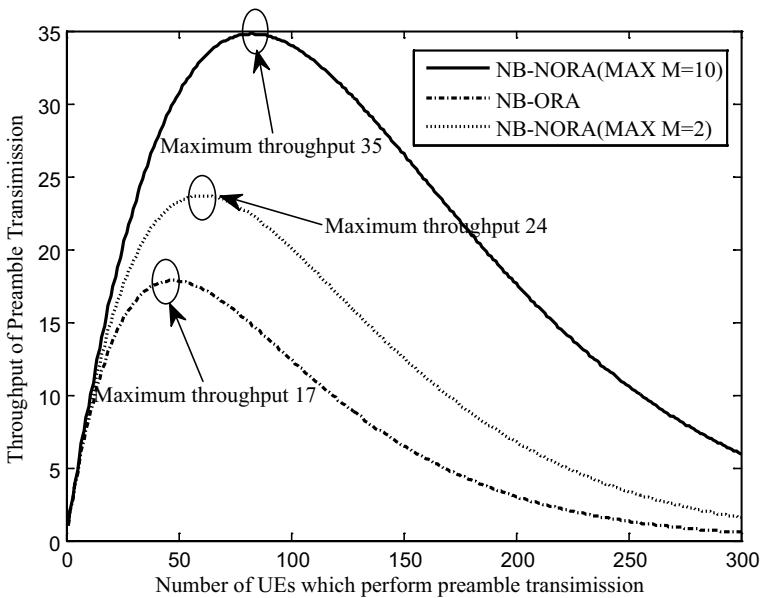


Fig. 2 MSG1 theoretical throughput with 0–1 distribution

3.2.1 NB-NOMA Uplink Power Control for MSG3

For uplink NOMA, SIC receiver requires diverse arrived power to distinguish multiplexed terminals. To obtain the diverse arrived power [13], a power back-off scheme is proposed for uplink NOMA transmission. Define ρ as the power back-off step of the target received power, the transmit power of the i th terminal in a NOMA set is expressed by Eq. (7)

$$p_i = \min\{p_{\max}, p_T - (i - 1)\rho + 10 \log_{10}(M_i) + \omega PL_i\} \tag{7}$$

where p_{\max} is the maximum transmit power. M_i is 1/4 for 3.75 kHz subcarrier spacing and {1, 3, 6, 12} for 15 kHz subcarrier spacing. p_T is the target arrived power in NB-ORA. PL_i is the downlink path loss estimated by the terminal in dB, parameter ω is the path loss attenuation factor of fractional transmission power control. NPUSCH uses full path loss compensation, so $\omega = 1$. Equation (7) denotes that the arrived power of NOMA terminals is gradually degraded with a step of ρ . This design is beneficial to cancel the co-channel interferences successively.

Since all terminals in a NB-NORA set share the same resource block (NPUSCH only occupies one RB), the difference between p_i and $p_j(j > i)$ can be written as Eq. (8),

$$p_i - p_j = PL(i) - PL(j) + (j - i)\rho \tag{8}$$

and Eq. (8) can be expressed in watt by Eq. (9),

$$\frac{p_i}{p_j} = \frac{PL(i)}{PL(j)} \cdot 10^{\frac{(j-i)\rho}{10}} = \frac{I_i^2}{I_j^2} \cdot 10^{\frac{(j-i)\rho}{10}} \tag{9}$$

A terminal with a large path loss is assigned a larger order step, so its arriving power is smaller than other terminals. This design helps to reduce power consumption when the terminal is far away from the BS, especially, in the cell edge range. The power back-off order value in NB-NORA group is decided according to the TA. With a larger TA will be assigned a larger order value, which indicates that the corresponding received power is smaller. Assuming the order of i th terminal is prior to the j th terminal, the MSG3 on the BS satisfies the expression Eq. (10)

$$p_i \|h_i\|^2 > p_j \|h_j\|^2 \tag{10}$$

where $\|h_i\|^2 = \frac{|g_i|^2}{I_i^2}$, $\|h_j\|^2 = \frac{|g_j|^2}{I_j^2}$, Substituting (9) into (10), we have Eq. (11)

$$|g_i|^2 > |g_j|^2 \cdot 10^{\frac{(j-i)\rho}{10}} \tag{11}$$

when $\rho = 0$, Eq. (11) becomes $|g_i|^2 > |g_j|^2 (i < j)$. Note that the lower bound of ρ is 0, so we take $|g_i|^2 > |g_j|^2 (i < j)$ as a condition to cover all possible values of ρ .

3.2.2 Separation Probability of NB-NORA Terminals

After analyzing the uplink power control for MSG3, the achievable data rate of the m th terminal is defined R_m . \hat{R}_{RA} is the target data rate of the detectable MSG3. $Z_m = \{R_m < \hat{R}_{RA}\}$

represent that the BS cannot detect the MSG3 from m th terminal. Z_m^C is the complementary set of Z_m . The event Z_i^C and Z_j^C are mutually independent when $i \neq j$. The outage probability of the m th terminal can be expressed as Eq. (12)

$$P_m^{out} = 1 - P(Z_1^C \cap Z_2^C \cap \dots \cap Z_{m-1}^C \cap Z_m^C) = 1 - \prod_{j=1}^m P(Z_j^C) \tag{12}$$

If the current decoded message is not the last signal, the probability of event Z_m^C is given by Eq. (13)

$$\begin{aligned} P(Z_m^C) &= 1 - P\{R_m < \hat{R}_{RA}\} \\ &= 1 - P\left\{ \log\left(1 + \frac{P_m |h_m|^2}{\sum_{i=m+1}^M P_i |h_i|^2 + \sigma^2}\right) < \hat{R}_{RA} \right\} \end{aligned} \tag{13}$$

If the current decoding message is the last Multiplexed MSG3 the probability of event Z_m^C is given by Eq. (14)

$$\begin{aligned} P(Z_M^C) &= P\left\{ \log\left(1 + \frac{P_M |h_M|^2}{\sigma^2}\right) \geq \hat{R}_{RA} \right\} \\ &= 1 - P\left\{ |g_M|^2 < \frac{\psi l_M^2 \delta^2}{P_M} \right\} \\ &= 1 - \int_0^{\beta_M} f_M(x) dx_M \\ &= 1 - \int_0^{\beta_M} M(1 - F(x_M))^{M-1} f(x_M) dx_M \\ &= e^{-\frac{-M\beta_M}{2\mu^2}} \end{aligned} \tag{14}$$

where $f_M(x) = M(1 - F(x_M))^{M-1} f(x_M)$ is derived by analyzing order statistics under the condition of $|g_M|^2 \leq \dots \leq |g_2|^2 \leq |g_1|^2$, $\psi = 2^{R_{RA}} - 1$ and $\beta_M = \frac{\psi l_M^2 \delta^2}{P_M}$.

3.2.3 Number of Terminals Successfully Transmitting MSG3

The number of terminals which transmitted MSG3 successfully in the cell is defined as Eq. (15)

$$\begin{aligned} U_{rS}^{MSG3} &= \sum_{j=1}^{M^r} j P(\max\{Z_j^C\}) \\ P(\max\{Z_j^C\}) &= P\{P(\max\{Z_j^C\}) \neq 0, P(\max\{Z_{j+1}^C\}) = 0\} \\ U_{NORA}^{MSG3} &= \sum_{r=1}^N U_{rS}^{MSG3} \end{aligned} \tag{15}$$

where M^r represents the number of terminals in the sets of NB-NORA-RAR with r elements. $P(\max\{Z_j^C\})$ represents the probability that j th multiplexing terminal can be

successfully decoded in the NB-NORA. U_{rS}^{MSG3} indicates the mathematical expectation of the number of successfully separated MSG3 which use the same preamble r .

Comparing with the NB-ORA scheme, the number of successfully separated MSG3 in NB-ORA can be obtained as Eq. (16)

$$U_{ORA}^{Msg3} = \sum_{r=1}^N U_{rS}^{Msg3} \tag{16}$$

It is hard to get a closed-form of $P(Z_j^C)$ when the value of j is large [13]. The closed-form expression of the last step of Eqs. (12) and (15) is hard to get. This paper will give a simulation analysis of the performance in the next section.

4 Performance Evaluation

4.1 Simulation Throughput of MSG1

The MSG1 throughput of NB-NORA comparing NB-ORA is simulated in this section with following parameters. The preamble selection is based on discrete uniform distribution probability model. The cell radius is 2500 meters. RDS is 1us. The number of preambles is 48.

From Fig. 3, In NB-NORA, the MSG1 throughput is rapidly increased at first. Its maximum throughput is approximately twice that of NB-ORA, which is the same as it under 0–1 distribution in Fig. 2. However, under the potential access congestion at the burst

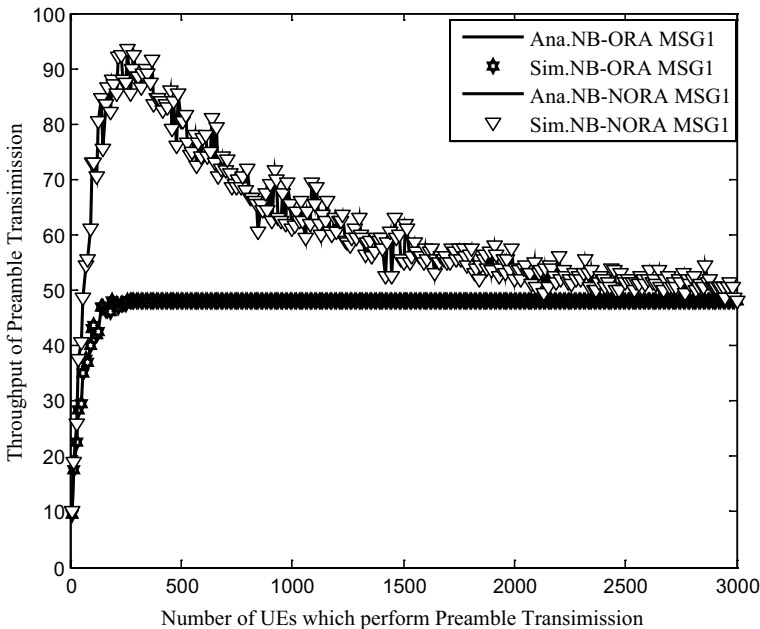


Fig. 3 Simulation throughput of MSG1 with uniform distribution

scenarios in NB-IoT (For example, power failure recovery scenarios) the MSG1 throughput will decrease along with the increase of the number of accessing terminals. The throughputs of NB-NORA and NB-ORA are similar when the number of terminals is large enough, however, preambles in NB-NORA can be effectively decoded to increase the successful access of MSG1. When the number of simultaneous access terminals is very large, NB-NORA mechanism will lose its advantage, this is because the BS will not be able to distinguish multiplexing terminals based on differences in arrival times with too many preambles launching simultaneously and hence the non-orthogonal scheme will fail.

4.2 Simulation Throughput of RAP

4.2.1 MSG3 Success Access Probability

It is hard to get a closed-form of Eqs. (7) and (8). Therefore, the number of terminals with transmitting MSG3 successfully is simulated in Fig. 5 with following parameters. Assumed $G_l = 1$, $\mu = 1$, $\lambda = 0.15$, $R_{ORA} = 1.6$, $\rho = 5$ dB, QPSK modulation.

Figure 4 shows the number of successful transmitted terminals when the number of multiplexed terminals is $m=3, 5, 7$, and 9 , respectively. From Fig. 4, with the increase of the maximum of arrival SNR, the number of successfully transmitted terminals increases gradually. At the same time, when the number of multiplexing terminals is small, the number of separated terminals will increase with the increase of multiplexing terminals. However, as the number of multiplexing terminals increases, the terminal signal with a large power back-off order will be annihilated by noise, and the number of successfully separated terminals will stop rising.

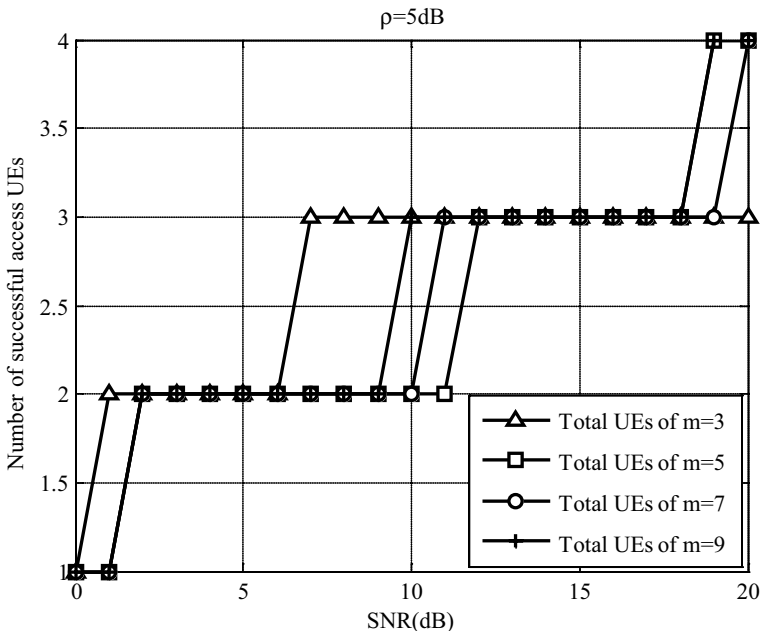


Fig. 4 Number of terminals successfully transmitting MSG3

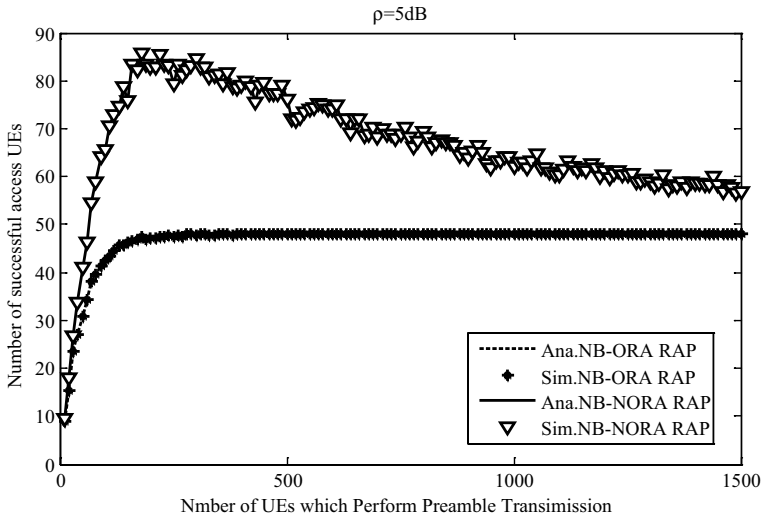


Fig. 5 Throughput of RAP

4.2.2 RAP Throughput with Different ρ

Figure 5 shows the throughput of narrowband RAP under both NB-NORA and NB-ORA when the step of power back-off is 5 dB. Figure 6 shows the difference in throughput of narrowband RAP at different size of power back-off step ρ .

From Fig. 5, the number of initial access successes rises rapidly and reaches its maximum throughput with increase of the number of initiated access when there are less accesses. At this time, the maximum throughput of NB-NORA can reach about 75% higher than that of NB-ORA. When the number of initiated access continue to increase, the maximum throughput of NB-ORA will be kept and it of NB-NORA will decline. That's because that too many multiplexed users make the BS unable to distinguish them according to arrival time. Furthermore, even if a large number of conflicting users are successfully separated, in the next step of multiplex MSG3 transmission, signals from users with large power back-off orders will be overwhelmed by channel noise. The SIC technology cannot be separated and decoded successfully. RA will not succeed. Therefore, the NB-NORA scheme eventually reduces to the level of orthogonal access. In general, when the number of terminals that perform RAP simultaneously is higher than the total number of available preambles, the NB-NORA mechanism can effectively alleviate the potential access congestion at the burst scenarios in NB-IoT.

Figure 6 shows the difference of throughput in NB-NORA when the power back-off step is 5 dB, 6 dB, and 7 dB respectively. Figure 6-1 shows the difference in RA throughput for back-off 6 dB and back-off 5 dB, when the number of terminals is less than 800. 6 dB throughput performance is significantly better than 5 dB performance; Fig. 6-2 shows the difference in RA throughput with 7 dB back-off and 5 dB back-off. Similarly, it can be seen that performances with 7 dB is better than that with 5 dB; Fig. 6-3 shows the difference in RA throughput with 7 dB back-off and 6 dB back-off. It can be seen that it with 7 dB is slightly lower than it with 6 dB. From those figures, when the power back off step is too small, the terminal with smaller order can't be separated and decoded successful. However,

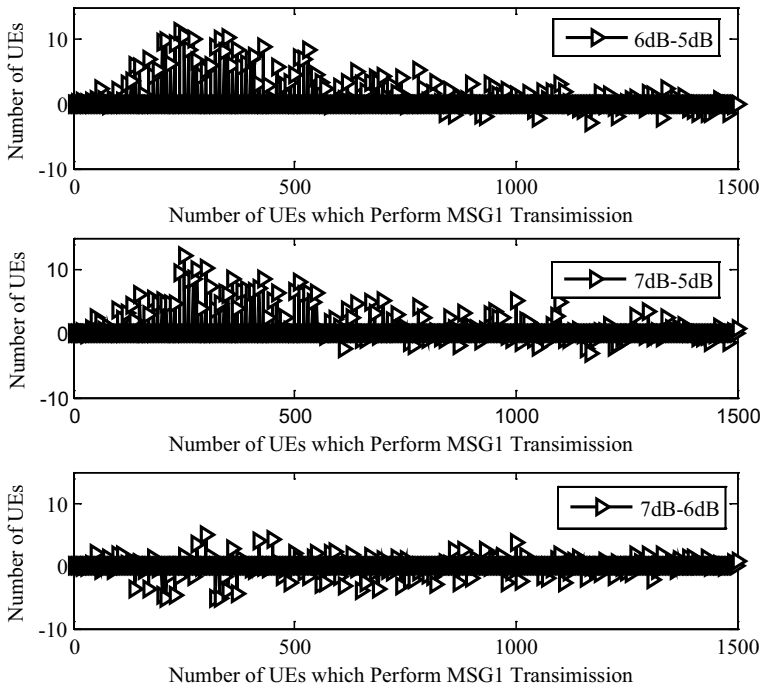


Fig. 6 RAP throughput difference of different power back-off steps

when the step length is too large, the transmission power of signal with big order is too small. Thus, the useful signal is buried by noise and cannot be successfully decoded.

5 Conclusion

In this paper, the NB-NORA mechanism was proposed to alleviate the potential access congestion at the burst scenarios in NB-IoT. Specifically, the locations of multiplexing terminals are utilized to realize MSG1 detection and NB-NORA-RARs reception. Furthermore, NOMA and SIC technologies are applied to the multiplexing MSG3 transmission, thus alleviates the demand for limited NPUSCH resources. The simulation results show that NB-NORA outperforms NB-ORA in term of RA throughput. Compared with NB-ORA, NB-NORA can increase the throughput of the RA process by more than 75%. However, the increase of terminals will lead to an explosion of terminal conflicts. It is difficult for the NB-NORA to separate MSG1s from different terminals. Furthermore, with a larger order, the transmit power of MSG3 is weaker, and signal will be buried by noise. The BS cannot decode it successfully, and the system throughput will gradually decrease to the NB-ORA mechanism.

Funding This work was supported by the National Natural Science Foundation of China (Grant No. 61701063) and China Scholarship Council.

Appendix

NB-NOMA System Model [13]

We assume a single-cell uplink transmission scenario, in which the evolved NodeB (eNB) is located at the center of the cell. The channel between the m th terminal and the eNB is denoted by h_m and $h_m = \frac{g_m}{l_m}$, where l_m and g_m denotes pathloss and Rayleigh fading channel gain, respectively. To simplify the analysis, l_m is modelled by Free-Space path loss model [18], i.e., $l_m = \left(\frac{\sqrt{G_t}\lambda}{4\pi d}\right)^2$, where G_t is the product of the transmit and receive antenna field radiation patterns in the line-of-sight (LOS) direction, and λ is the signal wave-length and d denotes the distance between terminal and eNB. The probability density function (PDF) of $|g_m|^2$ can be written as

$$f_{|g_m|^2}(x) = \frac{1}{2\mu^2} e^{-\frac{x}{2\mu^2}} \quad (17)$$

where μ is the variance of the normal distribution $N(0, \mu)$. Assuming that there are M terminals sharing the same uplink channel simultaneously, the received signal at eNB is given by

$$Y = \sum_{i=1}^M h_i \sqrt{p_i} s_i + n \quad (18)$$

where p_i and s_i are the transmit power and transmit messages from the i th terminal, respectively. n denotes the additive noise at eNB. In order to split the overlapped signals, SIC receiver is carried out at eNB. Before eNB detects the m th terminal's message, it decodes the prior i th ($i < m$) terminals' message first, then remove the message from its observation, in a successive manner. The rest ($M-m$) terminals' messages are regarded as interferences. As a result, the achievable data rate of the m th terminal is

$$R_m = \log \left(1 + \frac{p_m |h_m|^2}{\sum_{i=m+1}^M p_i |h_i|^2 + \sigma^2} \right) \quad (19)$$

Assuming \hat{R}_m is the target data rate of the m th terminal, then the event that eNB successfully detects the m th terminal's message can be defined as

$$R_m \geq \hat{R}_m \quad (20)$$

Note that the pre-condition of (13) is $R_m \geq \hat{R}_m (i < m)$ i.e., eNB needs to correctly decode the prior ($m-1$) terminals' messages before detecting the m th terminal's message, where R_i and \hat{R}_i are the achievable data rate and the target data rate of the i th terminal, respectively.

References

1. GPP.TR 38.913 v.14.2.0. (2017). *Study on scenarios and requirements for next generation access technologies*.

2. ITU Doc.5D/TEMP/300-E, *Minimum Requirements Related to Technical Performance for IMT-2020 Radio Interface(s)*, <http://www.itu.int/pub/R-REP-M.2134-2008.2017>.
3. GPP.TS 36.211 v.14.2.0. (2017). *Evolved universal terrestrial radio access (E-UTRA): Physical channels and modulation*.
4. Rohde & Schwarz. (2016). Narrowband internet of things whitepaper. *White paper*.
5. Ratasuk, R., Vejlgard, B., Mangalvedhe, N., et al. (2016). NB-IoT system for M2M communication. In *Wireless Communications and networking conference* (pp. 428–432). IEEE. <https://doi.org/10.1109/wncn.2016.7564708>.
6. Chen, M., Miao, Y., Hao, Y., et al. (2017). Narrow band internet of things. *IEEE Access*, 5(99), 20557–20577.
7. Chen, M., Miao, Y., & Hao, Y., et al. (2016). *Technical specification group radio access network; evolved universal terrestrial radio access (E-UTRA); physical channels and modulation; (Release 13)*,” TS 36.211 V13.2.0.
8. Jiang, N., Deng, Y., Condoluci, M., et al. (2018). RACH preamble repetition in NB-IoT network. *IEEE Communications Letters*, 22(6), 1244–1247. <https://doi.org/10.1109/lcomm.2018.2793.274>.
9. Kim, T., Han, S. J., & Han, K. S. (2015). An enhanced random access scheme with spatial group based reusable preamble allocation in cellular M2M networks. *IEEE Communications Letters*, 19(10), 1714–1717. <https://doi.org/10.1109/LCOMM.2015.2473860>.
10. Benjebbovu, A. et al. (2013). System-level performance of downlink NOMA for future LTE enhancements. In: *Proceedings of IEEE Globecom workshop, Atlanta* (pp. 66–70).
11. Kim, B. et al. (2013). Non-orthogonal multiple access in a downlink multiuser beamforming system. In *Proceedings of IEEE Military Communication Conference, San Diego, CA* (pp. 1278–1283).
12. Sedaghat, M. A., & Müller, R. R. (2018). On user pairing in uplink NOMA. *IEEE Transactions on Wireless Communications*, 17(5), 3474–3486. <https://doi.org/10.1109/TWC.2018.2815005>.
13. Zhang, N., Wang, J., Kang, G., et al. (2016). Uplink nonorthogonal multiple access in 5G systems. *IEEE Communications Letters*, 20(3), 458–461. <https://doi.org/10.1109/LCOMM.2016.2521374>.
14. Liang, Y., Li, X., Zhang, J., et al. (2017). Non-orthogonal random access (NORA) for 5G networks. *IEEE Transactions on Wireless Communications*, 16(7), 4817–4831. <https://doi.org/10.1109/TWC.2017.2703168>.
15. Seo, J. B., Bang, C. J., & Hu, J. (2018). Non-orthogonal random access for 5G mobile communication systems. *IEEE Transactions on Vehicular Technology*, 67(8), 7867–7871. <https://doi.org/10.1109/TVT.2018.2825462>.
16. Stefania, S., Issam, T., & Matthew, B. (2011). *LTE—The UMTS long term evolution: From theory to practice*. Hoboken, NJ: Wiley.
17. Kim, T., Bang, I., & Dan, K. S. (2017). An enhanced PRACH preamble detector for cellular IoT communications. *IEEE Communications Letters*, 21(12), 2678–2681. <https://doi.org/10.1109/LCOMM.2017.2745543>.
18. Goldsmith, A. (2005). *Wireless communications*. Cambridge: Cambridge Univ. Press.

Publisher’s Note Springer Nature remains neutral with regard to jurisdictional claims in published maps and institutional affiliations.



Dan Wang (1981) received the Ph.D. degree in communication engineering from Chongqing University, Chongqing, China, in 2014. From 2006 to 2009, she worked in Chongqing Chongyou information technology. She joint Chongqing University of Posts and Telecommunications in 2009 and worked on a wide array of wireless communication technologies including TD-SCDMA, GSM, LTE.



Yuanyuan Qu (1994) received her B.S. degree in Chongqing University of Posts and Telecommunications, China, in 2016. She is studying for a master's degree from Chongqing University of Posts and Telecommunications, and worked on wireless communication technologies including LTE, 5G. Her specific research on random access process.



Yongli Fu (1993) received her B.S. degree in communication engineering from Tianjin Polytech University, China, in 2015. She is currently a master candidate in the field of NB-IoT protocol stack of Chongqing University of Posts and Telecommunications. Her research interests include 5G mobile network protocol stack as well as NB-IoT.



Yanjuan Yang (1992) received her bachelor's degree in communication engineering from Datong University, Shanxi Province, China in 2015. She is currently enrolled at Chongqing University of Posts and Telecommunications and will receive her master's degree in 2019. She is currently the main candidate for the NB-IoT physical layer. Her research interests include the 5G mobile network physical layer and NB-IoT.



Qirong Chen (1994) received the B.S. degree in Electronic and Information Engineering from Chongqing University of Technology, in 2016. He is currently a master candidate in the field of network security of Tactical Mobile Ad Hoc Networks of Chongqing University of Posts and Telecommunications.